ELSEVIER

S0032-3861(96)00894-4

Polymer Vol. 38 No. 13, pp. 3213–3221, 1997

0032-3861/97/$17.00 + 0.00

Simultaneous *in-situ* WAXS/SAXS and d.s.c. study of the recrystallization and melting behaviour of the α and β form of iPP

S. Vleeshouwers*

Centre for Polymers and Composites, Department of Chemical Engineering, Eindhoven University of Technology, PO Box 513, 5600 MB Eindhoven, The Netherlands
(Received 1 November 1995; revised 12 August 1996)

The behaviour of the α and β form of isotactic polypropylene (iPP) was studied during heating. The β form is usually found in iPP specimens that have been subjected to mechanical deformation, e.g. in injection moulded and extruded products. A sample containing a large fraction of the β form was obtained by doping with small amounts of quinacridone. To enable the study of recrystallization and melting of α and β iPP, simultaneous wide-angle X-ray scattering and small-angle X-ray scattering were used. Differential scanning calorimetry was used to facilitate correlations with previous work. Using this combination of techniques, several partial processes could be distinguished. Melting behaviour depended on the formation history. In samples formed at high cooling rates, best comparable to processing conditions, the melting of β crystals is followed by an absolute increase in α crystallinity. In the slowly cooled samples, α and β crystal lamellae melt independently on heating. Also the recrystallization of α crystals, resulting in lamellar thickening, was detected. © 1997 Elsevier Science Ltd.

(Keywords: α and β form polypropylene; synchrotron radiation; recrystallization)

INTRODUCTION

Isotactic polypropylene (iPP) can occur in several crystalline forms, denoted as α, β and γ phase. The monoclinic α form is the most stable and is well documented[1–4]. The β form has first been mentioned by Padden and Keith[1,2]. It is formed only at specific conditions, being thermodynamically less stable than the α form, but having a higher growth rate. It was recently determined as pseudo-hexagonal[5]. A third type of crystal structure, γ, is preferentially formed under pressure[6]. iPP crystallizes completely in the γ structure at pressures higher than 200 MPa[7]. It has an orthorhombic structure with non-parallel chains[8,9]. If iPP is quenched from the melt to low temperatures, a combination of a glass and a disordered (mesomorphic) phase is formed, which still has a helix conformation, the helices being parallel to each other on a local scale. Upon heating at atmospheric pressure, β, γ and the mesomorphic phase transform to the stable α form[10–12].

Of all crystal structures, the α form is the most common. However, in many applications of iPP the β form can be present in considerable amounts. In samples that have been subjected to high orientation or deformation in the melt, the β form can be found[13–16]. Injection moulded and extruded iPP samples usually show a skin-core morphology. The β structure is located in the skin of these samples[11,17,18]. Having a higher growth rate, the β form can also be promoted with respect to the α form by specific crystallization conditions: high cooling rates[4], high crystallization temperatures[1,2] or large temperature gradients[19,20].

Besides via orientation or specific crystallization conditions, the β phase can be obtained via crystallization in the presence of special nucleation agents[21,22]. A well-known nucleation agent is the dye quinacridone. In concentrations above 1 ppm (parts per million, 10^{-4} w%) it promotes the β phase in iPP cooled from the melt. A fraction of up to 90% β phase can be obtained by optimizing parameters as nucleation agent concentration, maximum melt temperature and iPP type[22]. The formation of samples via this route offers a way to study the β crystal structure in bulk amounts in homogeneous samples.

It is reported that mechanical properties, stability and physical properties of β-iPP differ from α-iPP. In compression moulded specimens, β-iPP is shown to have a lower modulus, a lower yield stress and a higher elongation at break, i.e. an enhanced ductility[23]. Varga reports differences in properties for blends of α and β type of iPP with other polymers, e.g. with polyethylene[24]. Shi[25] reports a lower yield stress and earlier strain hardening in the tensile deformation for the β structure.

The transformation of the less stable β phase into the α phase upon heating or annealing is since long known[1,2,4]. Many publications on the melting and annealing behaviour of iPP by differential scanning calorimetry (d.s.c.)[15,26–30] are available. Usually several peaks are detected, which can be explained as melting and recrystallization and/or transformation of the present phases. Extensive studies by d.s.c. on the melting

* Present address: Philips Semiconductors, MOS4YOU, Gerstweg 2, 6534 AE Nijmegen, The Netherlands

behaviour of the β phase have been reported by Varga[26]. He recognized the occurrence of partial processes, i.e. the melting and recrystallization process and the particular recrystallization and melting behaviour of the β phase[27]. After cooling of β crystals to low temperatures ($\leq 100°C$) after crystallization, subsequent heating resulted in a $\beta \rightarrow \alpha'$ transition, followed by melting of α'-iPP. The prime ($'$) denotes a phase formed via recrystallization. If the temperature had not been below 100°C, β melted directly, or after recrystallization $\beta \rightarrow \beta'$ if the heating rate was chosen sufficiently low ($< 10°C\,min^{-1}$). These observations were later confirmed and extended by Lotz *et al.*[30], using d.s.c. and optical microscopy. They concluded that an $\alpha \rightarrow \beta$ growth transition exists at about 100°C. During cooling secondary crystallization of α crystals within the β sperulites will result in dispersed α overgrowth of β sperulites[27,30]. Varga first found evidence for a high-temperature $\beta \rightarrow \alpha'$ transition, which takes place during heating[26,27]. A further report on the $\beta \rightarrow \alpha'$ transformation was based on micro X-ray diffraction[31]. Samuels and Yee[31] concluded that the $\beta \rightarrow \alpha'$ recrystallization must take place via the liquid phase because of the considerable differences in unit cell of both structures. Based on cold rolling experiments, Asano[32] concluded that the transformation $\beta \rightarrow \alpha'$ during this process takes place via unfolding, melting and recrystallizing and not via breaking up lamellar stacks into blocks that are later incorporated into new lamellae.

In addition to d.s.c. and conventional X-ray techniques, *in-situ* wide and small angle scattering (WAXS/SAXS) studies can give considerable additional information on structural changes in iPP during heating. Only limited *in-situ* WAXS studies of the behaviour of β during heating have been reported[33,34]. Forgásc used synchrotron radiation for WAXS experiments on one β-iPP sample doped with 300 ppm nucleation agent quinacridone[33]. The sample was melted at 200°C and subsequently quenched in cold water. He recorded one 60 s-spectrum every 2 min during heating at $2°C\,min^{-1}$. The β crystals disappeared between 130–150°C, in favour of the α crystallinity. During heating the total crystallinity decreased, except for the period during the $\beta \rightarrow \alpha'$ transformation, where it was approximately constant. The conclusions based on these experiments were later confirmed by the experiments of Garbarczyk *et al.*[34] and the d.s.c. experiments by Varga[26,27,30].

In the present investigation simultaneous WAXS and SAXS is used during the heating and melting of iPP samples in which both α and β crystals are present. Samples with different nucleation agent concentration and different crystallization (cooling) conditions have been investigated. The transformation process $\beta \rightarrow \alpha'$ and $\alpha \rightarrow \alpha'$, lamellar thickening and the melting process are resolved. A correlation with d.s.c. data is made.

EXPERIMENTAL

Materials

The iPP used in this study is injection moulding grade StamylanP 13E10 (DSM, Geleen, The Netherlands). Values of $M_w = 500\,kg\,mol^{-1}$, $M_n = 100\,kg\,mol^{-1}$ were supplied by the manufacturer. As a nucleation agent the dye quinacridone, commercial name Hostaperm Red E3B, was used, kindly provided by Hoechst.

Pellets of iPP were powdered and nucleation agent was added in a concentration of 300 ppm. The powder was vigorously shaken until a homogeneous dispersion was obtained. Further dilution steps with pure PP powder resulted in concentrations of nucleation agent of 30, 3 and 0.3 ppm. The powder was processed in a small extruder during 2 min at 230°C. Discs with a thickness of 0.5 mm were cut from the thread-like extrudate (ϕ 3 mm). As a reference also an iPP sample without nucleation agent was prepared the same way, via powdering and extrusion.

D.s.c.

A Perkin–Elmer DSC-7 equipped with a robot was used for the d.s.c. measurements. The temperature calibration of the d.s.c. was performed using the melting peak of indium, at $10°C\,min^{-1}$. The d.s.c. was used for preparation of samples for the SAXS/WAXS experiments and, besides, for (conventional) d.s.c. experiments. Samples were prepared by melting discs cut out of the extrudate in the d.s.c. at 200°C during 15 min, followed by controlled cooling at -2 or $-50°C\,min^{-1}$ and recovering the polymer discs from the pans. Part of the samples were analysed by d.s.c. About 5 mg was measured at a heating rate of $5°C\,min^{-1}$. Nitrogen was used as a flow gas.

Samples are coded using the amount of nucleation agent and the cooling rate, e.g. sample 3/−2 is the sample with 3 ppm nucleation agent, formed by cooling at $2°C\,min^{-1}$ from the melt.

SAXS/WAXS

Simultaneous small and wide angle X-ray scattering (SAXS and WAXS) experiments were performed at beamline 8.2 of the SRS at SERC Daresbury Laboratory, Warrington, UK. Details of the beamline set up have been reported previously[34]. A small angle multiwire quadrant detector is used with a camera length of 3.5 m. The arc shaped wide angle detector (radius 20 cm) is placed with the sample in its focus. To minimize the scattering due to air, a vacuum chamber is placed between sample and detector. Monochromatic radiation with a wavelength of 1.5 Å is used. The calibration of the detectors was performed by measuring the scattering of wet collagen for the small angle detector, and by assignment of the strong reflections of iPP for the wide angle detector.

The prepared disc-like sample (ϕ 3 mm, thickness 0.5 mm) was placed between two thin mica sheets and placed on the heating block of a Linkam hot-stage. The sample was held in contact with the heating block by a light weight aluminium holder, equipped with a screw to assure good thermal contact. The heating cell with sample holder had been calibrated under a light microscope using well-defined melting standards. This resulted in a correction between the monitored temperature and the real sample temperature.

In each experiment a new sample was heated from room temperature to 90°C at $30°C\,min^{-1}$, and from 90°C to temperatures above the melting point at a nominal $2°C\,min^{-1}$. During these experiments the first spectrum was recorded at room temperature before the heating was started. Further, one spectrum was recorded every degree difference in temperature, i.e. every 30 s, starting at the nominal temperature 100°C, i.e. 97°C after correction. During these and other experiments it was

determined that no significant changes occurred in the WAXS spectra at low temperatures, which validated the choice of 97°C as a temperature at which the recordings were started. Recorded spectra were corrected for background scattering by the camera, hot-stage and mica windows of the sample holder, and for positional alinearity of the small angle detector.

Data analysis

Integration of the area under the Lorentz corrected intensity $q^2I(q)$ in the small angle regime vs q is performed between $q = 0$ and $q = 0.08$ to obtain the relative invariant Q'. This quantity is used as a measure for the total scattering power. The position of the peak of the Lorentz corrected intensity $q^2I(q)$ gives the long period L within the lamellar stacks. The one-dimensional correlation function has been calculated from the small angle scattering data. The analysis in terms of the quasi-two phase model is explained by Strobl[35] and gives values for the long period L, the length of the blocks L_1 and L_2 and the crystallinity in the lamellar stacks.

RESULTS AND DISCUSSION

D.s.c.

Results of d.s.c. experiments, obtained on samples cooled at 2°C min^{-1}, are presented in *Figure 1*. All samples show two melting endotherms. A gradual increase in peak temperatures of both endotherms is observed with increasing nucleation agent content. This can be explained by the corresponding crystallization temperatures recorded by d.s.c. during formation of the samples, see *Table 1*. With increasing nucleation agent content, the peak position of the crystallization exotherm shifts 11°C to higher temperatures. This causes the melting temperatures to shift to higher values.

The samples with 0 and 0.3 ppm nucleation agent only contain small amounts of the β phase (≤ 5%) and consist mainly of the α phase, as will be shown later in the WAXS experiments. The samples with the high nucleation agent content (3 and 30 ppm) contain a larger fraction of β (see *Table 1*). The two peaks in the d.s.c. experiments are caused by melting of the β and α phases, respectively. This is supported by d.s.c. experiments with larger scan speeds, up to 50°C min^{-1} [36]. In these d.s.c. traces, a constant ratio of the two peak areas is found. In case the second peak would be caused by melting of recrystallized material, its size would decrease with increasing scan speed, due to suppression of the recrystallization process[37].

The sample without nucleation agent cooled at −50°C min^{-1} (sample 0/−50) again shows two endothermic peaks, at 158°C and 164°C, see *Figure 2*. The low temperature peak is situated at much higher temperatures, compared to the same material cooled at 2°C min^{-1}, shown in *Figure 1*. Due to the high cooling rate the crystallization took place as much as 29°C lower (see *Table 1*). Accordingly, the recrystallization (of mainly α phase) starts at lower temperatures and is spread out over a larger temperature trajectory. The melting and recrystallization processes completely mask each other. The two endotherms are caused by the melting of still present, originally formed α crystals, and of recrystallized α′ crystals. The occurrence of (partial) recrystallization is confirmed by d.s.c. scans with larger scan speeds. An increase of the relative area of the first peak, compared to the second peak, is found[36]. At scan speeds ≥ 20°C min^{-1} the high temperature peak has completely disappeared.

The samples with 0.3, 3 and 30 ppm nucleation agent and cooled at −50°C min^{-1} show a melting behaviour distinctly different from the samples cooled at 2°C min^{-1}, which is also shown in *Figure 2*. At 143–152°C two small

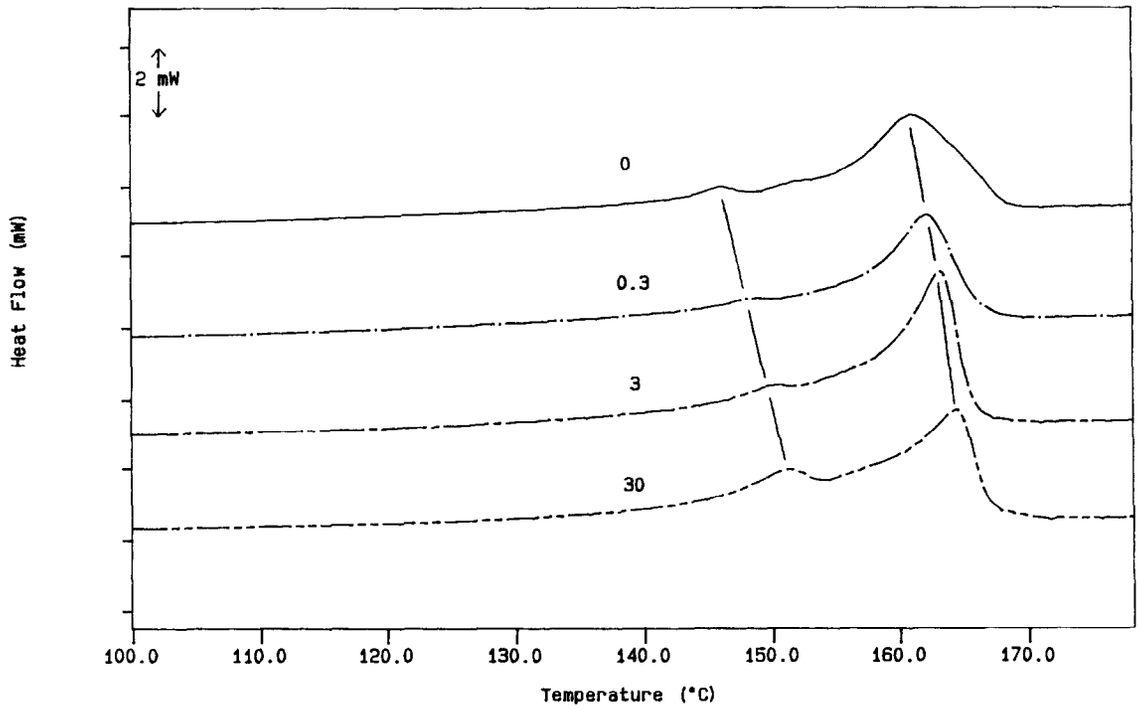

Figure 1 D.s.c. traces for samples cooled at −2°C min^{-1}, scanned at 5°C min^{-1}. Samples with nucleation agent concentration in ppm as indicated in the figure

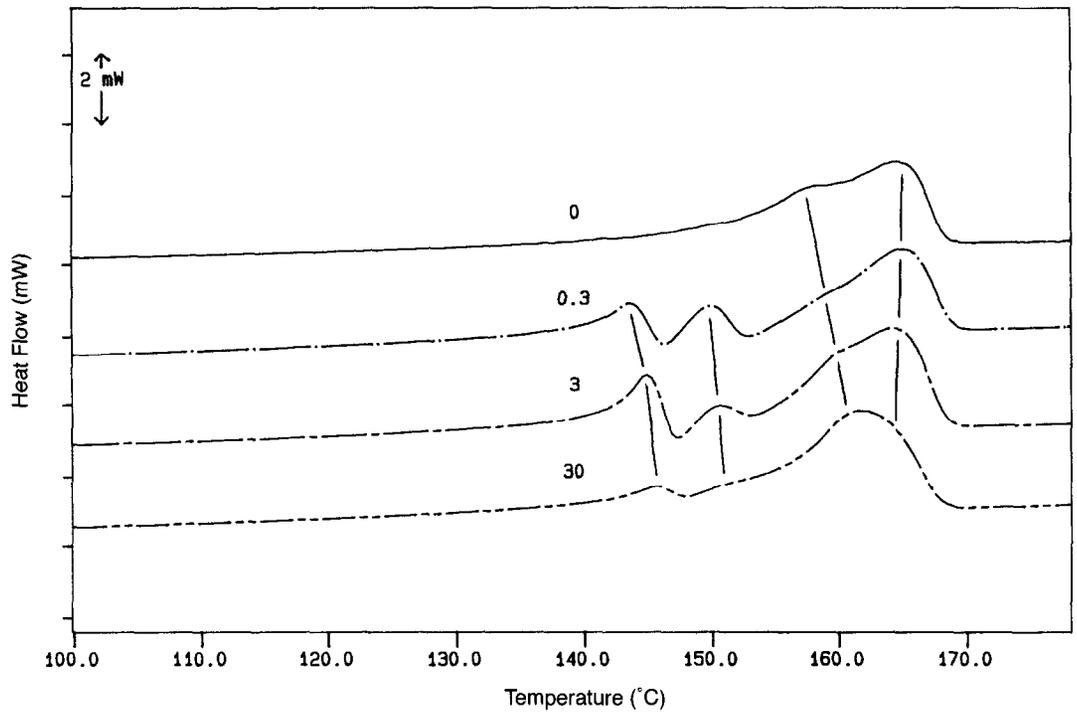

Figure 2 As *Figure 1*, but for samples cooled at $-50°C\,min^{-1}$

endotherms can be seen, separated by an exotherm. This exothermic process causes the d.s.c. trace even to cross the base line in samples 0.3/−50 and 3/−50. At temperatures around 165°C an endotherm is found, accompanied by an endothermic shoulder at about 160°C. In the 30/−50 sample, the peak at 160°C has a shoulder at 165°C. The process of melting of β and partly recrystallizing as α′ results in two endothermic and one exothermic peak below 152°C. This is in accordance with results by Varga[26,27]. Besides this process, the recrystallization of α also takes place, resulting in two melting peaks, one of the original α, one of the recrystallized α′. The higher the concentration of nucleation agent, the larger the α melt peak (around 160°C) and the less important the α′ melt peak (around 165°C). Also the position of the first peak shifts to higher temperatures. The position of the melting peak of recrystallized α′ is found to be constant. This is in accordance with the fact that the position of a melting peak of recrystallized material does not depend on sample history, but only on scan speed[37]. Due to the presence of the nucleating agent crystallization starts at a higher temperature. Thus the lamellar thickness is greater, and thermal stability is higher. The crystals melting at a higher temperature will have less time to recrystallize into the α form. This causes the α′ peak to be less pronounced. The d.s.c. experiments show distinctly a dual melting behaviour of lamellae α and α′ at high temperatures.

To obtain the fraction of crystallinity by integration of the total peak area in d.s.c. thermograms is difficult and not unambiguous[38]. This method results in values different from those obtained by X-ray techniques. To get a relative indication of crystallinity integration was performed between 100 and 180°C. These scans were recorded at $20°C\,min^{-1}$ heating rate to get an optimal sensitivity. Data are presented in *Table 1*. They show clearly that by slow cooling, a larger overall crystallinity is obtained.

WAXS

In *Figure 3* the WAXS data for sample 0.3/−50 are given at a heating rate of $2°C\,min^{-1}$ as a series of 80 spectra, each taken after a 0.9°C temperature increase. This results in a so-called surface plot. The important peaks characteristic of the α phase can be found at scattering angles 2θ of 14° (1 1 0), 17° (0 4 0), 18.5° (1 3 0), 21° (1 1 1) and 22° ($\bar{1}$ 3 1 and 0 4 1)[4]. The β phase can be detected by peaks at 16° (3 0 0) and 21° (3 0 1)[4]. The relative amounts of α and β are determined by the ratio of the sum of intensities of the α peaks (1 1 0), (0 4 0) and (1 3 0) and of the β (3 0 0) peak[4]. The fraction $\beta/(\alpha+\beta)$ for all samples, determined from the first spectrum, is given in *Table 1*. The total area under these peaks is in principle a measure for the bulk crystallinity. Due to lack of calibration absolute values for crystallinity are impossible to give. The relative amounts of α and β, however, can reliably be determined. From these data it can be seen that the used nucleation agent is an effective promotor for crystallization in β phase, making it possible to obtain homogeneous bulk samples with high β content. At high cooling rates, the optimal concentration nucleation agent shifts to lower values. The highest β content was obtained by a combination of 0.3 ppm nucleation agent and a cooling rate of $50°C\,min^{-1}$.

The concentration nucleation agent and the percentage β phase do not seem to influence the total crystallinity as determined from the area under the d.s.c. curves, see *Table 1*.

The peak area of the most important peaks of sample 0.3/−50 is presented in *Figure 4*. Upon heating the amount α is constant at temperatures below 135°C, whereas a small amount of β-iPP melts. As a result the overall crystallinity slightly decreases. At 135–147°C the β peak-intensity decreases until all β is gone. Meanwhile the α peak intensities grow in an absolute sense. It shows that during the disappearance of β lamellae, α lamellae are formed.

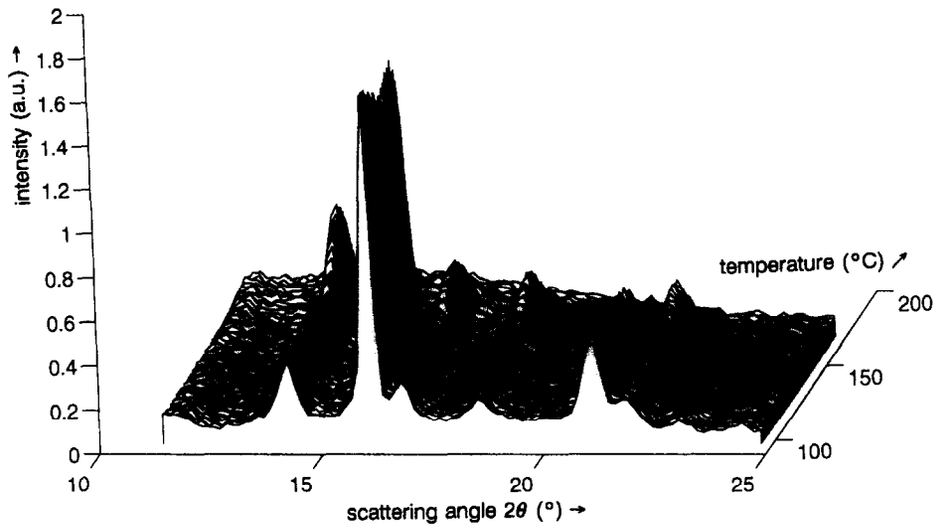

Figure 3 The intensity of wide-angle scattering *versus* diffraction angle 2θ and *versus* temperature. Sample 0.3/−50, recorded during heating at 2°C min^{-1}

Table 1 Characterization of used samples

Cooling rate (°C min^{-1})	Conc. nucl agent (ppm)	Cryst. temp. T_c [a] (°C)	Melt enthalpy ΔH [b] (J g^{-1})	Fraction $\beta/(\alpha+\beta)$ [c] (−)	Long period L [d] (Å)	Local cryst. x_{loc} [d] (−)
2	0	117	100	≤ 0.05	168	0.73
	0.3	122	101	≤ 0.05	180	0.76
	3	126	103	0.17	190	0.78
	30	128	103	0.27	194	0.80
50	0	88	92	≤ 0.05	148	0.73
	0.3	93	90	0.67	188	0.80
	3	96	93	0.57	192	0.78
	30	100	96	0.18	164	0.77

[a] Peak temperature of d.s.c. exotherms during cooling
[b] Determined from d.s.c. scans at 20°C min^{-1} heating rate
[c] Determined from WAXS data at 97°C
[d] Determined from the correlation function at 97°C

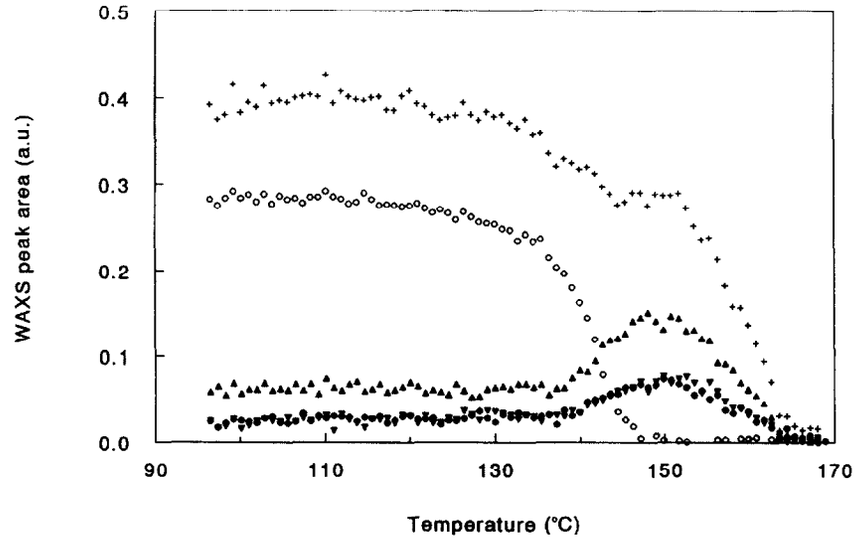

Figure 4 Peak areas of α and β peaks vs temperature for sample 0.3/−50, integrated from WAXS data; $\alpha_{(110)}$ (▲); $\alpha_{(040)}$ (●); $\alpha_{(130)}$ (▼); $\beta_{(300)}$ (○); $\alpha_{(110)} + \alpha_{(040)} + \alpha_{(130)} + \beta_{(300)}$ (+)

After all β has melted, the overall crystallinity stays constant from 147–152°C. The lamellae now present are of the α type, to a large extent crystallized at high temperatures. At 152°C these lamellae start to melt until at 170°C all crystallinity has disappeared. These results extend the d.s.c. results presented earlier, as the behaviour of α and β type crystals can be followed separately.

When the melting behaviour of all samples is compared, it is found that besides the already presented sample 0.3/−50, also sample 3/−50 shows an increase in α crystallinity after the melting of β, as seen from the WAXS intensities. From the d.s.c. data it could be expected that also sample 30/−50 would melt in a similar way, because the same endotherms and exotherms are found as for samples 0.3/−50 and 3/−50. However, no increase in α crystallinity was found from 135–150°C for sample 30/−50. This might be caused by the fact that only a fraction of the small percentage β-iPP present (18%) is expected to transform into α. The crystallization of this sample took place around 100°C, i.e. the temperature at which a transition from β to α crystallization occurs[30]. This may have caused the formation of a different type of crystals than formed at higher crystallization temperatures, and as a result, different recrystallization and melting behaviour. The other samples that contain β in reasonable amounts, cooled at 2°C min^{-1}, i.e. 3/−2 and 30/−2 behave as illustrated in *Figure 5* for sample 3/−2. The β crystals melt below 150°C. The β melting is not accompanied by an increase in α crystallinity. The α peak intensities decrease gradually until at 170°C all crystallinity has vanished. Thus it is noted that depending on the cooling rate during crystallization, the melting and/or recrystallization of β takes place via a different process.

SAXS

The SAXS data for sample 0.3/−50 are presented as a surface plot in *Figure 6*, where the Lorentz corrected intensity is plotted. It is clear that during the heating process, both the location of the maximum and the intensity of the peak change. This behaviour can be seen more clearly in *Figure 7*, where the long period L, calculated from the position of the maximum, is plotted vs temperature. In the same figure, the long period determined via the correlation function is also plotted. As can be expected, the results via the two methods show very good agreement. L is found to increase during heating at an ever increasing rate. All samples show this type of behaviour. Values for L for all samples, obtained from the first spectrum at 97°C, are given in *Table 1*. It is found that an increase of nucleation agent from 0 to 30 ppm causes an increase of the long period for the samples crystallized at 2°C min^{-1}: L increases from 168 Å to 194 Å. An increase of cooling rate can be expected to be accompanied by a decrease in L. This is clear for the samples 0/−2 and 0/−50, containing basically only α crystals: L decreases from 168 Å to 148 Å. However, the samples with the high β content, samples 0.3/−50 and 3/−50, show an anomalous behaviour. These samples have lamellar thicknesses L = 188 Å and 192 Å, respectively, comparable to those of the samples crystallized during slow cooling, i.e. 0.3/−2 and 3/−2 (L = 180 Å and 190 Å, respectively). Taking into account the high cooling rates, samples 0.3/−50 and 3/−50 possess relatively thick crystalline lamellae. If one assumes that the crystallization of α and β takes place in independent stacks and does not interfere, one might expect for the long period in these samples the α lamellae to have the same lamellar thickness L = 148 Å as in the 0/−50 sample which contains only α type of lamellae. This might indicate that the long period in the β lamellae is substantially higher than in the α lamellae.

The area under the Lorentz corrected small angle peak is called the relative invariant $Q \propto x(1-x)$, with x the average bulk crystallinity in the sample. Q' is plotted in *Figure 8* for sample 0.3/−50. A constant increase of Q' is found until 138°C. At this temperature the rate of increase suddenly grows. This increase accompanies the absolute growth of α crystallinity. Initially the sample is assumed to have a crystallinity larger than 0.5, in accordance with d.s.c. results. It is anticipated that the crystallinity decreases during heating, the maximum in Q' indicating that a crystallinity of 0.5 is reached. It can now be concluded that the crystallization of α′ cannot fully compensate the loss of crystallinity by melting of β. At 152°C this maximum is observed. At even higher temperatures, Q' decreases rapidly until it vanishes at

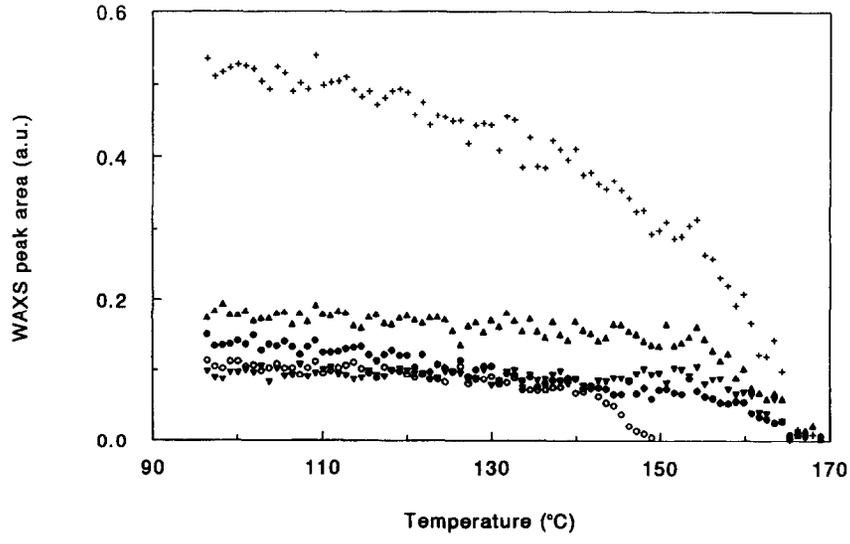

Figure 5 Peak areas of α and β peaks vs temperature for sample 3/−2, integrated from WAXS data; symbols as in *Figure 4*

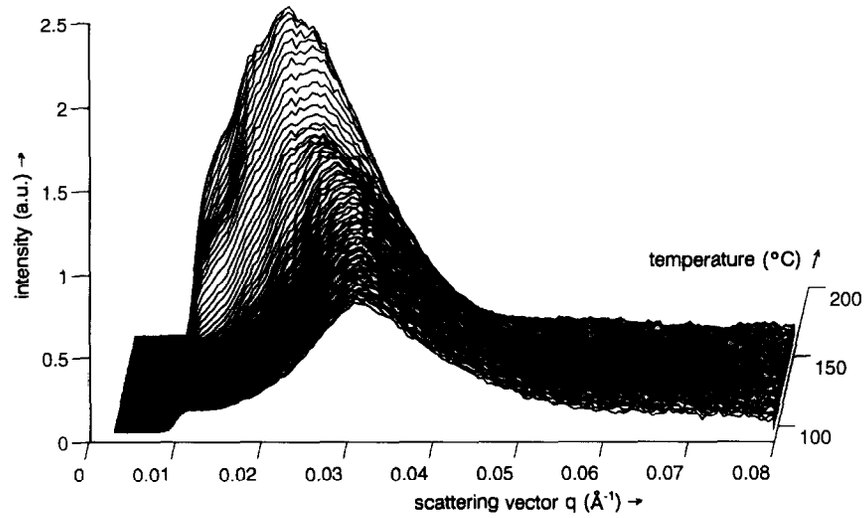

Figure 6 The Lorentz corrected intensity of small angle scattering vs scattering vector q and vs temperature. Sample 0.3/−50, during heating at 2°C min^{-1}

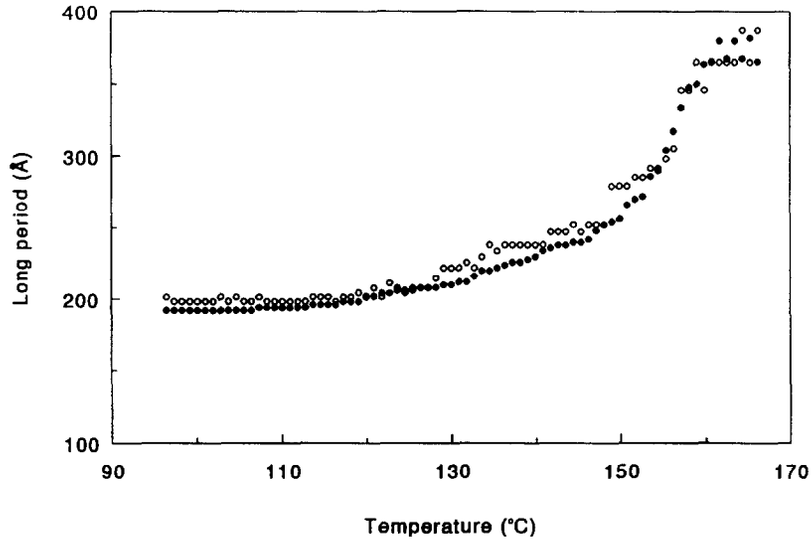

Figure 7 Long period L vs temperature for sample 0.3/−50, during heating at 2°C min^{-1}. Determined from Lorentz corrected small angle scattering (○) and correlation function (●)

temperatures where the crystals completely melt. All samples formed at a cooling rate of 50°C min^{-1} show this type of behaviour. It can be concluded that the crystallization of α' cannot fully compensate the loss of crystallinity by melting of β.

As an example of a slowly cooled sample, where α and β melt independently, the evolution of the invariant for sample 3/−2 is also plotted in *Figure 8*. Here the invariant gradually increases until the maximum. A decrease in the invariant above 152°C is found, due to melting of α lamellae.

In *Figure 9* the local crystallinity x_{loc}, determined from the correlation function, is plotted vs temperature for samples 0.3/−50 and 3/−2. It must be noted that whereas the bulk crystallinity x, determined from the invariant, is an average over the scattering volume, x_{loc} determined from the correlation function is an average over the scattering bodies, i.e. the crystal lamellae. If part of the crystals melt a decrease in x does not have to be accompanied by a decrease in x_{loc}. For sample 0.3/−50 a slow decrease of x_{loc} is found, until 135°C. Then, after being constant until 152°C, the local crystallinity increases at even higher temperatures. Samples that show this trend in x_{loc} are the samples cooled at high rates. In the slowly cooled sample 3/−2, x_{loc} decreases monotonically, starting at 120°C until it finally seems to increase close to the final melting process. This behaviour is also found for sample 30/ − 2.

General discussion

For the fast cooled iPP samples, the moderate increase of L, the small decrease of x_{loc} and the slight decrease of the bulk crystallinity x below 135°C are in agreement with the conclusion from WAXS data that a few (thin) β lamellae melt. In the d.s.c. experiments this is seen as a slight endothermic curvature of the baseline. Between 135–152°C, from the faster increase of Q' and the decrease in total WAXS area it can be concluded that the overall crystallinity decreases substantially. From d.s.c. and WAXS experiments the $\beta \rightarrow \alpha'$ recrystallization is clear in the β containing samples. WAXS and SAXS experiments indicate that the $\beta \rightarrow \alpha'$ transformation

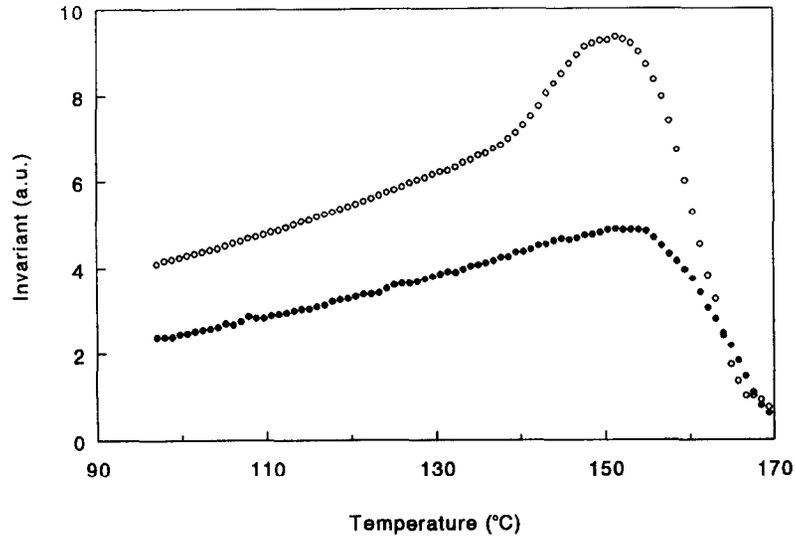

Figure 8 Relative invariant Q' vs temperature during heating at 2°C min^{-1}. Samples 0.3/−50 (○) and 3/−2 (●)

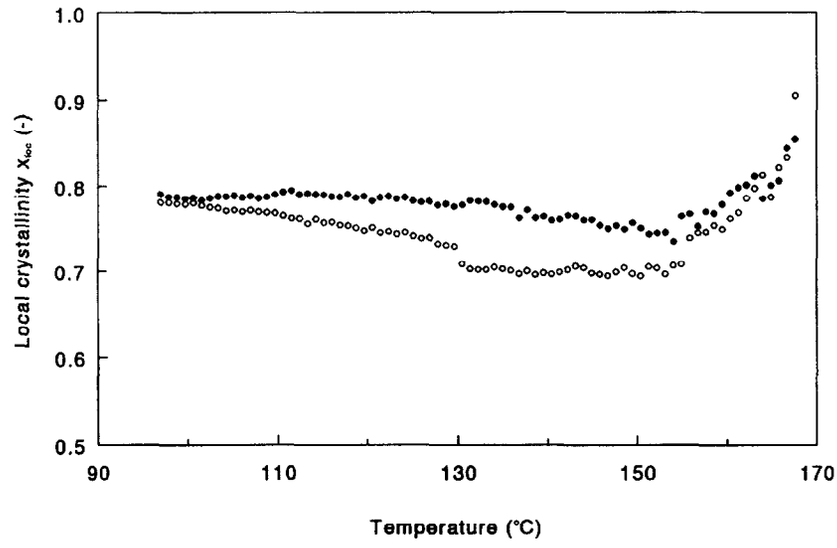

Figure 9 Local crystallinity x_{loc}, determined from the correlation function vs temperature, during heating at 2°C min^{-1}. Samples 0.3/−50 (○) and 3/−2 (●)

process is accompanied by a substantial increase in L and a decrease in overall crystallinity x. Lamellar stacks consisting of thin β lamellae melt completely. However, part of this material crystallizes again as α lamellae. These newly formed α lamellae are thicker than those originally formed, due to the high crystallization temperature. The d.s.c. trace of sample 0/−50 indicates that α lamellae also present with low melting point recrystallize in this temperature regime. At temperatures above 152°C α lamellae start to melt, starting with the ones being less perfect, leading to an increasing long period L and an increasing local crystallinity x_{loc}. Now the absolute intensity of the WAXS peaks also decrease. The dual melting process is clearly visible from the d.s.c. traces of samples cooled at 50°C min^{-1} as two separate melting peaks.

The question under which conditions $\beta \rightarrow \alpha'$ recrystallization occurs has been given attention before. According to Varga[27] this recrystallization process could be attributed to the formation of α-nuclei within the β spherulites during secondary crystallization at low temperatures. Lotz *et al.* showed that this formation is due to the low temperature growth transition from β to α[30]. During heating these nuclei are very effective promotors of α crystallization after melting of β, and, as a result, a $\beta \rightarrow \alpha'$ transformation takes place. If annealing has taken place above 100°C before cooling to low temperatures all material will crystallize as β during this annealing step and no α nuclei will be formed[28]. Subsequent heating will then show a $\beta \rightarrow \beta'$ process.

The experiments presented here are not fully comparable, because of the non-isothermal crystallization conditions. In general, the same explanation can still be applicable. However, no evidence for a $\beta \rightarrow \beta'$ recrystallization was found in the slowly cooled samples. Forgásc' *in-situ* WAXS data[33] are confirmed by the present data. The extension by simultaneous SAXS experiments and the use of a variety of samples has further explained the role of formation history and the melting behaviour of the α and β lamellae.

In this study a nucleation agent was used to obtain homogeneous samples with large β crystal content. Distinctly different melting behaviour of β crystals was detected depending on cooling rate. The samples formed at high cooling rates might be best compared to samples containing β crystallinity due to mechanical deformation.

ACKNOWLEDGEMENTS

We are grateful to Hoechst, the Netherlands, for providing the quinacridone. Beam time at Daresbury was provided under reference number 25/313. We thank NWO for financial support of the synchrotron experiments. A. Spoelstra, Prof. P. Lemstra and Prof. B. Lotz are acknowledged for their contributions.

REFERENCES

1. Padden, F. J. and Keith, H. D., *J. Appl. Phys.*, 1959, **30,** 1479.
2. Keith, H. D., Padden, F. J., Walter, N. M. and Wyckoff, H. W., *J. Appl. Phys.*, 1959, **30,** 1485.
3. Natta, G. and Corradini, P., *Nuovo Cimento*, 1960, **15,** 40.
4. Turner-Jones, A. Aizlewood, J. M. and Beckett, D. R., *Makromol. Chem.*, 1964, **75,** 134.
5. Meille, S. V., Ferro, D. R., Brückner, S., Lovinger, A. J. and Padden, F. J., *Macromolecules*, 1994, **27,** 2615.
6. Meille, S. V., Brückner, S. and Porzio, W., *Macromolecules*, 1990, **23,** 4114.
7. Nakafuku, C., *Polymer*, 1981, **22,** 1673.
8. Kardos, J. L., Christiansen, A. W. and Baer, E., *J. Polym. Sci.: A-2*, 1966, **4,** 777.
9. Lotz, B., Graff, S., Straupé, C. and Wittmann, J. C., *Polymer*, 1991, **32,** 2902.
10. Glotin, M., Rahalkar, R. R., Hendra, P. J., Cudby, M. E. A. and Wiilis, H. A., *Polymer*, 1981, **22,** 731.
11. Fleischmann, E., Zipper, P., Jánosi, A., Geymayer, W., Koppelmann, J. and Schurz, J., *Polym. Eng. Sci.*, 1989, **29,** 835.
12. O'Kane, W. J., Young, R. J., Ryan, A. J., Bras, W., Derbyshire, G. E. and Mant, G. R., *Polymer*, 1994, **35,** 1352.
13. Leugering, H. J. and Kirsch, G., *Angew. Makromol. Chem.*, 1973, **33,** 17.
14. Dragaun, H., Hubeny, H. and Muschik, H., *J. Polym. Sci., Polym. Phys. Ed.*, 1977, **15,** 1779.
15. Devaux, E. and Chabert, B., *Polym. Commun.*, 1991, **32,** 464.
16. Zipper, P., Jánosi, A., Wrentschur, E., Abuja, P. M. and Knabl, C., *Progr. Colloid Polym. Sci.*, 1993, **93,** 377.
17. Muschik, H. and Dragaun, H., *Progr. Colloid Polym. Sci.*, 1979, **66,** 319.
18. Wenig, W. and Herzog, F., *J. Appl. Polym. Sci.*, 1993, **50,** 2163.
19. Fujiwara, Y., *Colloid Polym. Sci.*, 1955, **253,** 273.
20. Lovinger, A. J., Jaime, O. C. and Gryte, C. C., *J. Polym. Sci., Polym. Phys. Ed.*, 1977, **15,** 641.
21. Leugering, H. J., *Makromol. Chem.*, 1967, **109,** 204.
22. Moos, K. and Tilger, B., *Angew. Makromol. Chem.*, 1981, **94,** 213.
23. Jacoby, P., Bersted, B. H., Kissel, W. J. and Smith, C. E., *J. Polym. Sci., Polym. Phys. Ed.*, 1986, **24,** 461.
24. Varga, J., Schulek-Tóth, F. and Mudra, I., *Macromol. Symp.*, 1994, **78,** 229.
25. Shi, G., Chu, F. Zhou, G. and Han, Z., *Makromol. Chem.*, 1989, **190,** 907.
26. Varga, J., Gábor, G. and Ille, A., *Angew. Makromol. Chem.*, 1986, **142,** 171.
27. Varga, J., *J. Therm. Anal.*, 1986, **31,** 165.
28. Varga, J. and Tòth, F., *Makromol. Chem. Makromol. Symp.*, 1986, **5,** 213.
29. Passingham, C., Hendra, P. J., Cudby, M. E. A., Zichy, V. and Weller, M., *Eur. Polym. J.*, 1990, **26,** 631.
30. Fillon, B., Thierry, A., Wittmann, J. C. and Lotz, B., *J. Polym. Sci., Polym. Phys. Ed.*, 1993, **31,** 1407.
31. Samuels, R. J. and Yee, R. Y., *J. Polym. Sci., Polym. Phys. Ed.*, 1972, **10,** 385.
32. Asano, T. and Fujiwara, Y., *Polymer*, 1978, **19,** 99.
33. Forgács, R., Tolochko, B. P. and Sheromov, M. A., *Polym. Bull.*, 1981, **6,** 127.
34. Bras, W., Derbyshire, G. E., Ryan, A. J., Mant, G. R., Felton, A., Lewis, R. A., Hall, C. J. and Greaves, G. N., *Nucl. Instr. Meth. Phys. Res.*, 1993, **A326,** 587.
35. Strobl, G. R. and Schneider, M., *J. Polym. Sci., Polym. Phys. Ed.*, 1980, **18,** 1343.
36. Vleeshouwers, S. Unpublished results, 1995.
37. Lemstra, P. J., Kooistra, T. and Challa, G., *J. Polym. Sci. A-2*, 1972, **10,** 823.
38. Wunderlich, B., *Macromolecular Physics*. Academic Press, New York, 1980.
39. Garbarczyk, J., Sterzynski, T. and Paukszta, D., *Polym. Commun.*, 1989, **30,** 153.